7726 *Inorg. Chem.* **2010**, *49*, 7726–7734
DOI: 10.1021/ic100527d

Inorganic Chemistry
Article

Reaction of Ru^{II} Diazafluorenone Compound with Nanocrystalline TiO_2 Thin Film

William B. Heuer,*,† Hai-Long Xia,‡ Maria Abrahamsson,‡ Zhen Zhou,‡,§ Shane Ardo,‡ Amy A. Narducci Sarjeant,‡ and Gerald J. Meyer*,‡

†*Chemistry Department, United States Naval Academy, Annapolis, Maryland 21402,*
‡*Departments of Chemistry and Materials Science and Engineering, Johns Hopkins University, 3400 North Charles Street, Baltimore, Maryland 21218, and* §*School of Physics, Peking University, Beijing 100871, China*

Received March 19, 2010

The Ru(II) compounds $[Ru(bpy)_2(mcbH)]^{2+}$ and $[Ru(bpy)_2(dafo)]^{2+}$, bpy is 2,2′-bipyridine where mcbH is 3-(CO_2H)-2,2′-bipyridine and dafo is 4,5-diazafluoren-9-one, were synthesized, characterized, and anchored to nanocrystalline mesoporous TiO_2 thin films for excited state and interfacial electron transfer studies. X-ray crystallographic studies of $[Ru(bpy)_2(mcbH)](PF_6)(Cl)$ revealed a long Ru−N distance to the unsubstituted pyridine ligand of mcbH. Reaction of $[Ru(bpy)_2(dafo)]^{2+}$ with TiO_2 thin films resulted in interfacial chemistry. The IR, ^1H NMR, UV−vis, and photoluminescence spectral data indicated a room-temperature ring-opening reaction of the dafo ligand of $[Ru(bpy)_2(dafo)]^{2+}$ that ultimately yielded a carboxylate group in the 3-position of bipyridine anchored to TiO_2. Comparative reactions of $[Ru(bpy)_2(mcbH)]^{2+}$ with TiO_2 were performed and support this conclusion. In regenerative photoelectrochemical solar cells with 0.5 M LiI/0.05 M I_2 in acetonitrile, photocurrent action spectra were observed for both sensitized materials. The incident photon-to-current efficiency (IPCE) was significantly lower for $Ru(bpy)_2(dafo)/TiO_2$, behavior attributed to a lower excited-state injection yield.

Introduction

The reaction chemistry that occurs when metal oxide semiconductor surfaces are reacted with Ru(II) bipyridyl compounds is of considerable importance in dye-sensitized solar cells.[1] Surface "linkers" are derived from the reactions of carboxylic acid,[2] silane,[3] phosphonic acid,[4] acetylacetonate,[5] or ether[6] functional group(s) placed on a ligated pyridine ring. In some cases, organic spacers placed between such functional groups and the pyridine ring have been used to control interfacial electronic interactions.[7] Ruthenium polypyridyl compounds with carboxylic acid groups give rise to the most efficient electron transfer and are by far the most commonly utilized.[1,2] The surface reaction chemistry is usually accomplished by overnight room temperature reactions of a mesoporous nanocrystalline (∼20 nm diameter, anatase) TiO_2 thin film with millimolar concentrations of Ru(II) compounds dissolved in organic solvents. Infrared studies have shown that after such reactions the Ru(II) compounds are present on the TiO_2 surface with the carboxylic acid functional groups in their carboxylate forms.[7] Therefore, a complication with carboxylic acid surface reactivity, and other Brønsted acidic functional groups, is that the acidic protons transferred to TiO_2 induce a Nernstian shift of the conduction and valence band edge energies away from the vacuum level. Such lowering of the conduction band edge may favor excited-state injection but can be undesirable and lead to poor open-circuit photovoltages and hence lower power conversion efficiencies in dye-sensitized solar cells.

The unwanted influence of surface protonation on the conduction band edge is exacerbated with ruthenium polypyridyl compounds that have multiple carboxylic acid groups, like N3, *cis*-$Ru(dcb)_2(NCS)_2$, or the so-called black dye, $Ru(tct)(NCS)_3$, where dcb is 4,4′-$(COOH)_2$-2,2′-bipyridine and tct is 4,4′,4″-$(COOH)_3$-2,2′:6′,2″-terpyridine.[8] For this reason, it is often necessary to precipitate these compounds at a specific pH so that only one of the carboxylic acid groups is protonated.[9] Isolation of a single product can be extremely tedious as the pK_a's of the carboxylic acid groups

*To whom correspondence should be addressed. E-mail: heuer@usna.edu (W.B.H.); meyer@jhu.edu (G.J.M.).

(1) O'Regan, B.; Grätzel, M. *Nature* **1991**, *353*, 737.
(2) Anderson, S.; Constable, E. C.; Dare-Edwards, M. P.; Goodenough, J. B.; Hamnett, A.; Seddon, K. R.; Wright, R. D. *Nature* **1979**, *280*, 571.
(3) Ghosh, P.; Spiro, T. G. *J. Am. Chem. Soc.* **1980**, *102*, 5543.
(4) Pechy, P.; Rotzinger, F. P.; Nazeeruddin, M. K.; Kohle, O.; Zakerrudin, S. M.; Humphry-Baker, R.; Grätzel, M. *J. Chem. Soc., Chem. Commun.* **1995**, 65.
(5) Heimer, T. A.; D'Arcangelis, S. T.; Farzad, F.; Stipkala, J. M.; Meyer, G. J. *Inorg. Chem.* **1996**, *35*, 5319.
(6) Zou, C.; Wrighton, M. S. *J. Am. Chem. Soc.* **1990**, *112*, 7578.
(7) Galoppini, E. *Coord. Chem. Rev.* **2004**, *248*, 1283.
(8) Nazeeruddin, M. K.; Péchy, P.; Renouard, T.; Zakeeruddin, S. M.; Humphry-Baker, R.; Comte, P.; Liska, P.; Cevey, L.; Costa, E.; Shklover, V.; Spiccia, L.; Deacon, G. B.; Bignozzi, C. A.; Grätzel, M. *J. Am. Chem. Soc.* **2001**, *123*, 1613.
(9) Nazeeruddin, M. K.; Zakeeruddin, S. M.; Humphry-Baker, R.; Jirousek, M.; Liska, P.; Vlachopoulos, N.; Shklover, V.; Fischer, C.-H.; Grätzel, M. *Inorg. Chem.* **1999**, *38*, 6298.

 Published on Web 08/11/2010

Scheme 1

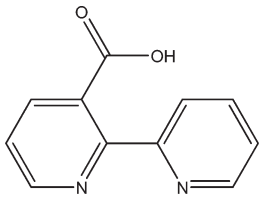

mcbH

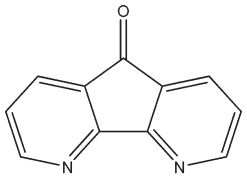

dafo

are very similar and, unless done carefully, a mixture often results. In addition, the introduction of carboxylic acid groups can significantly decrease the solubility of some compounds in the organic solvents optimized for the surface functionalization chemistry.[10] For many classes of dye molecules, carboxylic acid functional groups make chromatography, purification, and characterization much more difficult relative to the unsubstituted dye.

Hence it may be more desirable to anchor compounds to TiO_2 through a heterogeneous reaction of a neutral functional group that directly yields a molecular−semiconductor bond. An early example of this was reported for $[Ru(bpy)_2(deeb)]^{2+}$, where bpy is 2,2′-bipyridine and deeb is 4,4′-$(CO_2CH_2CH_3)_2$-2,2′-bipyridine.[11] The TiO_2 surface was found to saponify the ethyl ester groups and carboxylate-type binding was observed by attenuated total reflection Fourier-transform infrared (ATR-FTIR) spectroscopy.[11] Evidence for TiO_2 surface-catalyzed ester hydrolysis has been recently reported for copper bipyridyl compounds with methyl ester groups.[12] Surface functionalization with these compounds did not expose the TiO_2 surface to high concentrations of carboxylic acids. Another recent example of this was reported for perylene compounds that contained an anhydride group.[13,14] Reactions of this perylene compound with TiO_2 in alcohol−acetonitrile mixtures for 15 h led to a ring-opening reaction of the anhydride group and surface binding. Infrared analysis showed that the characteristic anhydride vibrations were absent for the surface-anchored perylene. This anhydride−TiO_2 reaction was later utilized for fundamental interfacial energetic studies where acidic protons were specifically unwanted.[15]

Here we report a new chemical reaction between TiO_2 and the neutral ketone group of a 4,5-diazafluoren-9-one (dafo) ligand coordinated to Ru(II), Scheme 1. Infrared, visible absorption, photoluminescence, and ^1H NMR measurements indicate that the surface-bound compound has a carboxylate functional group in the 3-position of a bipyridine ring. Comparative reactions of TiO_2 with $[Ru(bpy)_2(mcbH)]^{2+}$ support this conclusion, where mcbH is 3-(CO_2H)-2,2′-bipyridine. The commonly utilized surface reaction of TiO_2 with the carboxylic acid group in $[Ru(bpy)_2(mcbH)]^{2+}$ resulted in sensitized materials that were more optimal for photocurrent generation in regenerative solar cells than were sensitized materials prepared by reaction with the coordinated dafo ligand.

Experimental Section

Materials. All chemicals were reagent grade unless otherwise specified. Sulfuric acid (98%), diethyl ether (anhydrous), methanol (spectrophotometric grade), and sodium hydroxide were obtained from Fisher Scientific. Burdick and Jackson spectroscopic grade acetonitrile and distilled water were used as received. Ethanol and acetone were ACS reagent grade from Pharmco. Tetrabutylammonium perchlorate ($TBAClO_4$, electrochemical grade) was purchased from Fluka. Silver nitrate ($AgNO_3$) was from Bioanalytical Systems, Inc. Iodine (I_2, 99.8%), lithium iodide (LiI, 99.9%), and lithium hydroxide (LiOH, 98+ %) were obtained from Aldrich. Tetrabutylammonium iodide (TBAI, 99%) was purchased from Sigma. Deuterium oxide and sodium deuteroxide (30% in D_2O) were obtained from Cambridge Isotope Laboratories, Inc.

Preparations. The 4,5-diazafluoren-9-one (dafo) ligand as well as the $[Ru(bpy)_2(dafo)](PF_6)_2$ and $[Ru(bpy)_2(mcbH)](PF_6)_2$ coordination compounds were prepared and characterized as was previously described.[16,17]

Sensitized Colloidal Thin Films. Mesoporous thin films of anatase TiO_2 were prepared by previously described sol−gel procedures.[5] For most experiments, the thin films were placed in a pH = 12 aqueous solution (NaOH) for 1 h, rinsed with neat acetonitrile, and dried in air for 1 h. In some experiments, the pH = 12 aqueous solution was replaced by a pH = 1 aqueous solution (HCl). The pretreated TiO_2 thin films were reacted with millimolar concentrations of the Ru(II) compounds in acetonitrile for at least 24 h during which time the films turned deep red in color. The sensitized thin films were rinsed with acetonitrile prior to spectroscopic or electrochemical measurements. The surface coverages, Γ (mol cm^{-2}), were measured spectroscopically assuming that the extinction coefficient, ε (M^{-1} cm^{-1}), was the same in solution and on the surface. This value was used along with the modified Beer−Lambert law formula to calculate a macroscopic surface coverage by $A = \varepsilon \times \Gamma \times 1000$.

Spectroscopy. Photoluminescence. Steady-state photoluminescence (PL) spectra were obtained with a Spex Fluorolog spectrofluorometer that had been calibrated with a standard tungsten-halogen lamp using procedures provided by the manufacturer. For sensitized films, the excitation beam was directed 45° to the film surface, and the emitted light was monitored from the front face of the surface-attached sample and from the right angle for the sensitizer dissolved in solution. The acetonitrile was purged with argon gas for at least 15 min prior to PL measurements. Measurements at 77 K were performed in a 4:1 (v/v) EtOH/MeOH glass in a coldfinger Dewar.

Infrared Transmission. Attenuated Total Reflectance Fourier Transform infrared (ATR-FTIR) measurements were obtained with a Golden Gate Single Reflection Diamond ATR apparatus coupled to a Nexus 670 Thermo-Nicolet FTIR. Measurements were typically an average of 64 scans at 4 cm^{-1} resolution. For TiO_2 samples, unsensitized TiO_2 thin film served as the background. The spectra were not corrected for the wavelength-dependent path length.

Visible Absorption. Steady-state visible absorption data were obtained on a Varian Cary 50 in a 1 cm square quartz cuvette. For TiO_2 samples, the background was taken with a blank TiO_2 thin film, and the measurements were acquired by placing the slide in a solvent-filled cuvette.

(10) Hasselman, G. M.; Watson, D. F.; Stromberg, J.; Bocian, D. F.; Holten, D.; Lindsey, J. S.; Meyer, G. J. *J. Phys. Chem. B.* **2006**, *110*, 25430.
(11) Qu, P.; Meyer, G. J. *Langmuir* **2001**, *17*, 6720.
(12) Bessho, T.; Constable, E. C.; Grätzel, M.; Redondo, A. H.; Housecroft, C. E.; Kylberg, W.; Nazeeruddin, M. K.; Neuburger, M.; Schaffner, S. *Chem. Commun.* **2008**, 3717.
(13) Shibano, Y.; Umeyama, T.; Matano, Y.; Imahori, H. *Org. Lett.* **2007**, *9*, 1971.
(14) Li, C.; Yum, J.-H.; Moon, S.-J.; Herrmann, A.; Eickemeyer, F.; Pschirer, N. G.; Erk, P.; Schoneboom, J.; Mullen, K.; Grätzel, M.; Nazeeruddin, M. K. *ChemSusChem.* **2008**, *1*, 615.
(15) Cappel, U. B.; Gibson, E. A.; Hagfeldt, A.; Boschloo, G. *J. Phys. Chem. C* **2009**, *113*, 6275.
(16) Zheng, G. Y.; Wang, Y.; Rillema, D. P. *Inorg. Chem.* **1996**, *35*, 7118.
(17) Wang, Y.; Perez, W.; Z., G. Y.; Rillema, D. P. *Inorg. Chem.* **1998**, *37*, 2051.

Nanosecond absorption spectroscopy was obtained with an apparatus that has been previously described.[5] In short, excitation was accomplished with an 5 ns, 532 nm laser pulse from a Big Sky Brilliant Blue Nd:YAG laser normal to a 150 W pulsed Xe lamp probe beam. Samples were placed in a standard cuvette, and an atmosphere of Ar gas was maintained throughout the experiments.

Single Crystal X-ray Diffraction. Crystals suitable for X-ray measurements were obtained by slow diffusion of diethyl ether into 2−3 mL of CH_3CN solution of concentrated $[Ru(bpy)_2(mcbH)](PF_6)_2$ that contained 1 μL of a 1 M HCl aqueous solution.

The crystal was mounted in oil on the end of a glass fiber that was positioned in the diffractometer. The X-ray intensity data were measured at 110 K on an Oxford Diffraction Xcalibur3 system equipped with a graphite monochromator and a CCD detector. The final cell was obtained through a refinement of 16048 reflections to a maximum resolution of 0.72 Å. Data were collected via a series of 1.0° æ and ö scans. The frames were integrated with the Oxford Diffraction CrysAlisRED software package. A face-indexed absorption correction and an interframe scaling correction were also applied. The structure was solved using direct methods and refined using the Bruker SHELXTL (version 6.1) software package. Analysis of the data showed no sample decomposition.

^{1}H NMR Spectroscopy. Room temperature ^{1}H NMR spectra were recorded on Bruker 400Ultrashield and JEOL ECX-400 NMR instruments. Typically 10−20 sensitized thin films were placed in a pD = 10 deuterium oxide (NaOD) for 1 h. The dark red solutions were transferred to standard NMR tubes.

Electrochemistry. Cyclic voltammetry. A standard three-electrode arrangement consisting of a Pt button working electrode, a Pt gauze counter electrode, and an $Ag/AgNO_3$ non-aqueous reference electrode (0.1 M $AgNO_3$ in 0.1 M $TBAClO_4/CH_3CN$) was used for solution measurements in 0.1 M $TBAClO_4/CH_3CN$ electrolyte. Cyclic voltammetry of the sensitized TiO_2 thin film was performed in a similar manner except with the sensitized TiO_2/FTO films as the working electrode. The cyclic voltammetry experiments were carried out at room temperature under argon with a BAS model CV-50W potentiostat. The ferrocenium/ferrocene (Fc^+/Fc) potential was measured to be 67 mV versus $Ag/AgNO_3$ under these conditions.

Spectroelectrochemistry and Density of States Analysis. A standard three-electrode arrangement with a functionalized TiO_2 film deposited on FTO glass as the working electrode, a Pt mesh counter electrode, and an Ag/AgCl aqueous reference electrode (NaCl saturated) was assembled in a custom 1 cm square quartz cuvette with 0.1 M $LiClO_4$ in acetonitrile under an Ar atmosphere. The cuvette was placed in a Varian Cary 50 spectrophotometer, and the potential was controlled with a BAS CV-50W potentiostat. The potential was stepped by 50 mV, and the absorption spectrum was recorded. Each potential was held until at least 95% of the steady-state absorbance at 800 nm was reached. The density of states, as chemical capacitances in free energy, were calculated by conversion of absorption data to macroscopic surface coverage using the extinction coefficient of $TiO_2(e^-)$s of 850 M^{-1} cm^{-1} at 800 nm.

Photoelectrochemistry. Incident photon-to-current efficiency (IPCE) measurements were performed in a two-electrode sandwich cell arrangement as previously described.[5] Briefly, ~10 μL of a 0.5 M LiI/0.05 M I_2 acetonitrile electrolyte was sandwiched between a sensitized TiO_2 thin film electrode and a Pt-coated FTO electrode. The sandwich cell was illuminated through the sensitized TiO_2 film with quasi-monochromatic light from a 150 W Xe lamp coupled to an f/0.22 m monochromator. Photocurrents were measured with a Keithly model 617 digital electrometer. Incident irradiances were measured with a calibrated silicon photodiode from UDT Technologies. The IPCE was calculated using eq 1:

$$\mathrm{IPCE} = (1240 i_{ph})/(P\lambda) \quad (1)$$

Table 1. Crystallographic Data for $[Ru(bpy)_2(mcbH)](PF_6)(Cl)$

	$[Ru(bpy)_2(mcbH)](PF_6)(Cl)$
empirical formula	C31 H24 Cl F6 N6 O2 P Ru
formula weight	794.05
temperature (K)	110 K
wavelength (Å)	0.71073
crystal system	monoclinic
space group	$P2(1)/c$
a (Å)	10.1364(3)
b (Å)	30.9269(5)
c (Å)	11.2186(2)
B	96.316(2)
V (Å^3)	3495.54(13)
Z	4
D_{calc} (g/cm^3)	1.509
absorption coefficient (cm^{-1})	6.35
$F(000)$	1592
crystal size (mm)	0.5585 × 0.1323 × 0.0546
θ range for data collection (deg)	3.77 to 28.68
final R indices [$I > 2\sigma(I)$]	R1 = 0.0955
R indices (all data)	wR2 = 0.1712

Table 2. Selected Bond Distances (Å) and Bond Angles (deg) for $[Ru(bpy)_2(mcbH)](PF_6)(Cl)$

Ru(1)−N(5′)	1.970(15)	Ru(1)−N(4)	2.054(4)
Ru(1)−N(6)	1.996(10)	Ru(1)−N(2)	2.065(4)
Ru(1)−N(1)	2.053(4)	Ru(1)−N(5)	2.135(9)
Ru(1)−N(3)	2.053(5)	Ru(1)−N(6′)	2.231(17)
N(5′)−Ru(1)−N(6)	63.1(5)	N(4)−Ru(1)−N(2)	93.63(17)
N(5′)−Ru(1)−N(1)	97.7(5)	N(5′)−Ru(1)−N(5)	15.2(4)
N(6)−Ru(1)−N(1)	88.5(4)	N(6)−Ru(1)−N(5)	78.0(3)
N(5′)−Ru(1)−N(3)	106.2(5)	N(1)−Ru(1)−N(5)	95.7(3)
N(6)−Ru(1)−N(3)	168.6(3)	N(3)−Ru(1)−N(5)	91.6(3)
N(1)−Ru(1)−N(3)	97.35(17)	N(4)−Ru(1)−N(5)	92.0(3)
N(5′)−Ru(1)−N(4)	90.7(5)	N(2)−Ru(1)−N(5)	174.4(3)
N(6)−Ru(1)−N(4)	96.7(4)	N(5′)−Ru(1)−N(6′)	77.0(6)
N(1)−Ru(1)−N(4)	171.54(16)	N(6)−Ru(1)−N(6′)	13.8(4)
N(3)−Ru(1)−N(4)	78.78(18)	N(1)−Ru(1)−N(6′)	85.9(5)
N(5′)−Ru(1)−N(2)	164.2(5)	N(3)−Ru(1)−N(6′)	175.1(5)
N(6)−Ru(1)−N(2)	101.3(3)	N(4)−Ru(1)−N(6′)	97.5(5)
N(1)−Ru(1)−N(2)	78.74(17)	N(2)−Ru(1)−N(6′)	87.4(4)
N(3)−Ru(1)−N(2)	89.55(16)	N(5)−Ru(1)−N(6′)	91.8(4)

where i_{ph} is the photocurrent per unit area in μA/cm^2 at incident wavelength λ (nm) and P is the incident irradiance in μW/cm^2.

Results

The Ru(II) compounds $[Ru(bpy)_2(mcbH)](PF_6)_2$ and $[Ru(bpy)_2(dafo)](PF_6)_2$ were prepared in high yield following literature reports.[16,17] Crystals of $[Ru(bpy)_2(mcbH)](PF_6)(Cl)$ suitable for X-ray diffraction were obtained by slow diffusion of ether into an acetonitrile solution of the compound that was acidified with HCl. Crystallographic data and selected bond distances and angles are given in Tables 1 and 2. Two components were resolved that resulted from disorder of the mcbH ligand. The two components shown in Figure 1 have the carbons on the mcbH ligand numbered differently. The N(5)−Ru−N(6) angle of $[Ru(bpy)_2(mcbH)]^{2+}$ was 78.0(3)° for the mcbH ligand in major (60%) component, and N(5′)−Ru−N(6′) angle is 77.0(6)° for minor (40%) component. N(2)−Ru−N(1) and N(3)−Ru−N(4) for the two bpy ligands are 78.74(17)° and 78.78(18)°, respectively. The Ru−N(5) and Ru−N(6) distances were 2.135(9) Å and 1.996(10) Å for the major component whereas lengths of Ru−N(5′) and Ru−N(6′) were 1.970(15) Å and 2.231(17) Å for the minor $[Ru(bpy)_2(mcbH)]^{2+}$. All Ru−N distances to the unsubstituted bpy were in the range of 2.053−2.065 Å. Interestingly, the two

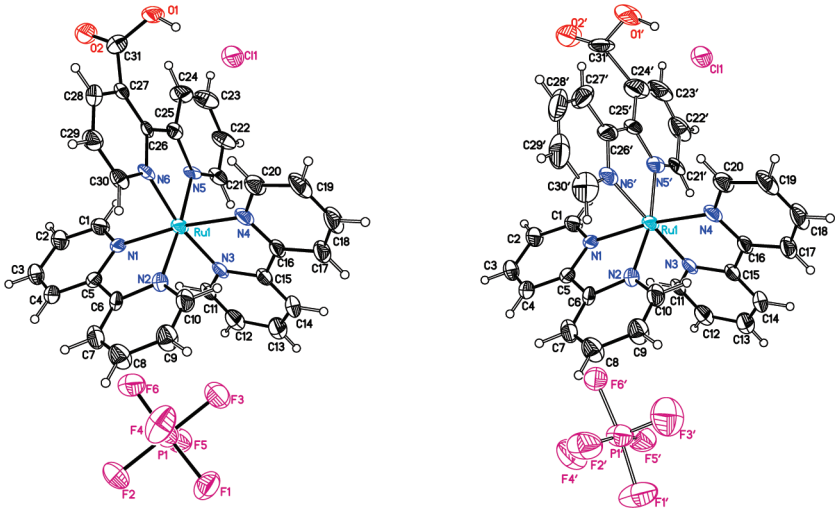

Figure 1. Major (60% left) and minor (40% right) component of $[Ru(bpy)_2(mcbH)](PF_6)(Cl)$ established by X-ray crystallography.

Table 3. Visible and IR Spectroscopic and Redox Properties for the Ru Compounds and Ru/TiO_2

	IR (cm^{-1}) [a]		absorption max. (nm) [b]		$E_{1/2}$ ($Ru^{III/II}$)[c] (V, vs $Ag/AgNO_3$)		$E_{1/2}$ ($Ru^{III/II*}$)[d] (V, vs $Ag/AgNO_3$)	
	solid	TiO_2	CH_3CN	TiO_2	CH_3CN	TiO_2	CH_3CN	TiO_2
$[Ru(bpy)_2(dafo)]^{2+}$	1741	1606	438	434 (s)	1.03	0.96	*e*	−1.2
	1605	1371		454				
$[Ru(bpy)_2(mcbH)]^{2+}$	1725	1606	450	434 (s)	0.95	0.94	−1.2	−1.2
	1604	1378		454				

[a] IR frequencies ±4 cm^{-1}; pure solid compounds measured as PF_6^- salts. [b] The MLCT absorption maxima where (s) indicates a shoulder peak. [c] Half-wave reduction potentials measured by cyclic voltammetry in 0.1 M $TBAClO_4/CH_3CN$. [d] Excited state reduction potentials calculated by eq 2. [e] No detectable PL was observed in CH_3CN precluding the calculation of $E_{1/2}(Ru^{III/II*})$.

pyridine rings of the mcbH ligand are essentially coplanar with a dihedral angle of $< 3°$ with the carboxylic acid hydrogen in position to form a hydrogen bond to the chloride anion.

The compounds were characterized by attenuated total reflection Fourier transform infrared (ATR-FTIR) spectroscopy and showed expected vibrations in the 1300−1550 cm^{-1} region from the bipyridine rings and intense IR bands in 1700−1750 cm^{-1} due to the C=O functional groups, Table 3.[18] An intense band at 1741 cm^{-1} for $[Ru(bpy)_2(dafo)]^{2+}$ was assigned to the CO stretch of the ketone group. $[Ru(bpy)_2(mcbH)]^{2+}$ displayed an intense band at 1725 cm^{-1} assigned to the COO asymmetric stretch of the carboxylic acid group.[18] Treatment of $[Ru(bpy)_2(mcbH)]^{2+}$ with NaOH yielded $[Ru(bpy)_2(3\text{-carboxylate-bpy})]^+$, that displayed bands at 1596 and 1375 cm^{-1}, assigned to asymmetric and symmetric COO stretches, respectively.

The compounds were found to bind to the mesoporous nanocrystalline TiO_2 thin films by overnight reactions in acetonitrile solution, and the resultant derivatized films are abbreviated $Ru(bpy)_2(dafo)/TiO_2$ and $Ru(bpy)_2(mcbH)/TiO_2$ herein. Unless otherwise stated, the films were pretreated with aqueous base before reaction with the Ru(II) compounds. For a large number of samples, the saturation surface coverages were in the range of $(1-5) \times 10^{-8}$ mol cm^{-2} for both compounds. The ATR-FTIR spectrum of $Ru(bpy)_2(mcbH)/TiO_2$ showed bands at 1606 cm^{-1} and 1378 cm^{-1}, Figure 2a. The corresponding spectrum of $Ru(bpy)_2(dafo)/TiO_2$ was remarkably similar with bands at 1606 cm^{-1} and 1371 cm^{-1}, Figure 2b. Notably absent in the spectrum of $Ru(bpy)_2(dafo)/TiO_2$ was the band assigned to the ketone of the parent compound at 1741 cm^{-1}. When the TiO_2 thin film was first pretreated with pH = 1 aqueous solution, $[Ru(bpy)_2(dafo)]^{2+}$ was found to bind to TiO_2, but in low surface coverage. The ketone band at 1741 cm^{-1} was observed for the acid-pretreated samples, Figure 2c.

Intense metal-to-ligand charge-transfer (MLCT) absorption bands were observed for the ruthenium compounds in solution and when anchored to TiO_2 thin films immersed in acetonitrile, Figure 3a and Table 3. The broad MLCT absorption maximum red-shifted from 438 to 454 nm after $[Ru(bpy)_2(dafo)]^{2+}$ had reacted with TiO_2.

Visible light excitation of $[Ru(bpy)_2(mcbH)]^{2+}$ in acetonitrile resulted in room temperature photoluminescence (PL), while no significant PL was observed from $[Ru(bpy)_2(dafo)]^{2+*}$ under the same conditions. Time resolved PL decay of $[Ru(bpy)_2(mcbH)]^{2+*}$ was well described by a first-order kinetic model with an excited-state lifetime, τ, of 560 ns. Both compounds were photoluminescent with well-resolved vibronic structure at 77 K in a 4:1 (v/v) ethanol/methanol glass, Figure 3b. The spectrum of $[Ru(bpy)_2(mcbH)]^{2+*}$ was in good agreement with previously reported 77 K data in 2-(CH_3)-THF/CH_2Cl_2, although the vibronic structure was better defined in the alcohol glass utilized here.[17] Excited-state decay was first-order at 77 K with τ = 4.6 μs for $[Ru(bpy)_2(mcbH)]^{2+*}$ and τ = 5.3 μs for $[Ru(bpy)_2(dafo)]^{2+*}$. Interestingly, room temperature PL was observed for $Ru(bpy)_2(dafo)/TiO_2$ and $Ru(bpy)_2(mcbH)/TiO_2$ thin films immersed in acetonitrile, Figure 3b inset.

The Ru(II) compounds in fluid solution and anchored to the TiO_2 thin films displayed quasi-reversible $Ru^{III/II}$ redox chemistry by cyclic voltammetry at scan rates of 20−100 mV/s,

(18) Deacon, G. B.; Phillips, R. J. *Coord. Chem. Rev.* **1980**, *33*, 227.

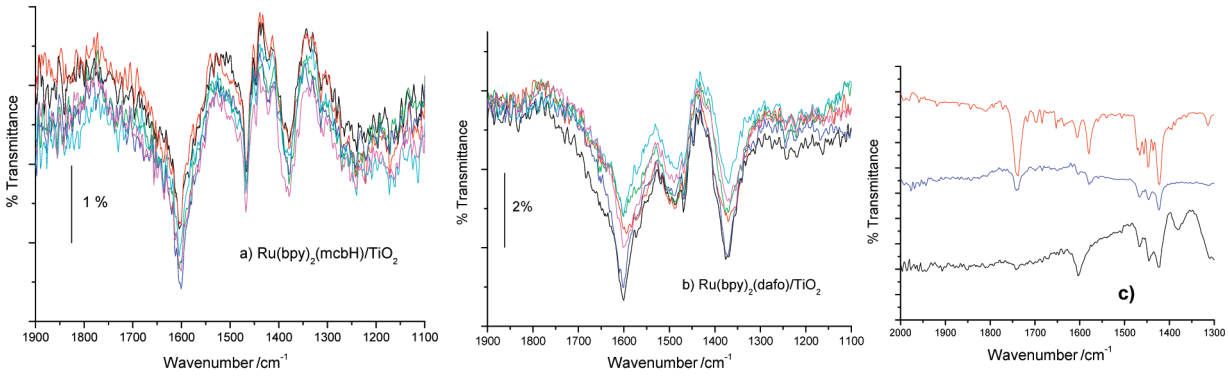

Figure 2. Attenuated total reflection Fourier transform infrared (ATR-FTIR) spectra of (a) $Ru(bpy)_2(mcbH)/TiO_2$ and (b) $Ru(bpy)_2(dafo)/TiO_2$. Spectral data from six representative TiO_2 thin films with different surface coverages are shown. Panel (c) displays comparative ATR-FTIR spectra of $[Ru(bpy)_2(dafo)](PF_6)_2$ (upper, red) and for the same compound anchored to acid (middle, blue), and base (lower, black) pretreated TiO_2. The spectra represent an average of 64 scans at ± 4 cm^{-1} spectral resolution.

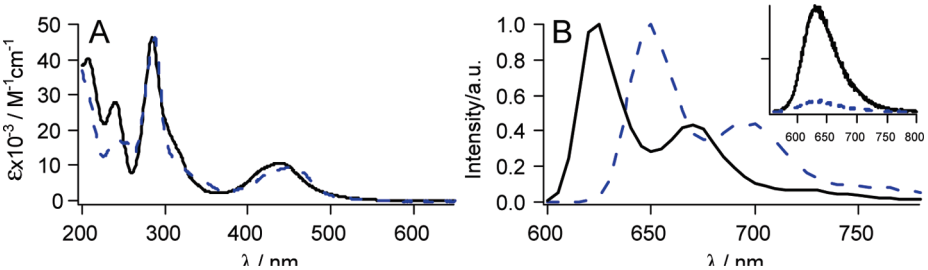

Figure 3. (a) UV−visible absorption spectrum of $[Ru(bpy)_2(mcbH)](PF_6)_2$ (solid line) and $[Ru(bpy)_2(dafo)](PF_6)_2$ (dashed line) immersed in acetonitrile at room temperature. (b) The 77 K PL spectra of the indicated compounds in a 4:1 (v/v) EtOH/MeOH glass. Inset is steady state PL spectra of $Ru(bpy)_2(mcbH)/TiO_2$ (solid line) and $Ru(bpy)_2(dafo)/TiO_2$ (dashed line) thin films immersed in argon-saturated acetonitrile at room temperature.

Table 3. The redox chemistry was termed quasi-reversible because the anodic and cathodic currents were approximately equal but the peak-to-peak separation was greater than 100 mV.[19] The half-wave potentials, $E_{1/2}(Ru^{III/II})$, were calculated as the average of the peak oxidation and reduction potentials. The excited-state reduction potentials, $E_{1/2}(Ru^{III/II*})$, were estimated by eq 2,

$$E_{1/2}(Ru^{III/II*}) = E_{1/2}(Ru^{III/II}) - \Delta G_{es} \qquad (2)$$

Here ΔG_{es} is the free energy stored in the thermally equilibrated MLCT excited state. This energy was approximated with a tangent line drawn on the high energy side of the corrected room temperature photoluminescence spectra. The calculated excited-state reduction potentials are included in Table 3.

Pulsed 532 nm laser excitation of $[Ru(bpy)_2(mcbH)]^{2+}$ in CH_3CN resulted in absorption difference spectra that were characteristic of an MLCT excited state, Figure 4. Positive absorptions were observed in the ultraviolet and at long wavelengths along with a bleach of the MLCT absorption band. The excited state decayed cleanly to ground-state products with maintenance of isosbestic points (at 408 and 513 nm) and first-order kinetics, $\tau = 560$ ns. No long-lived absorption transients were observed after pulsed-light excitation of $[Ru(bpy)_2(dafo)]^{2+}$ in acetonitrile consistent with an excited state lifetime < 10 ns.

The absorption difference spectrum observed after pulsed-light excitation of $Ru(bpy)_2(mcbH)/TiO_2$ or $Ru(bpy)_2(dafo)/$

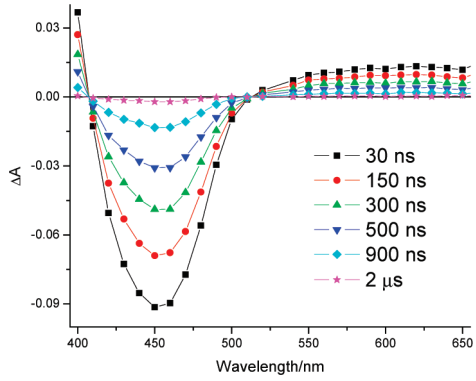

Figure 4. Absorption difference spectra measured at the indicated delay times after pulsed 532 nm light excitation of $[Ru(bpy)_2(mcbH)](PF_6)_2$ dissolved in argon-purged acetonitrile.

TiO_2 thin films immersed in CH_3CN was similar to that observed for $[Ru(bpy)_2(mcbH)]^{2+*}$ but lacked the absorption band in the UV region and the longer wavelength absorption was significantly red-shifted, Figure 5. The observed transients returned cleanly to ground-state products on a millisecond time scale with maintenance of isosbestic points at 400 and 540 nm. The absorption difference spectra were reasonably assigned to an interfacial charge-separated state composed of an electron in TiO_2 and the oxidized ruthenium compound. The appearance of this state could not be time-resolved consistent with $k_{inj} > 10^8$ s^{-1}. The magnitude of the absorbance change, and hence the excited-state injection yields on a nanosecond time scale, was consistently 2−3 times larger for $Ru(bpy)_2(mcbH)/TiO_2$ under these conditions.

(19) Bard, A. J.; Faulkner, L. R. *Electrochemical Methods: Fundamentals and Applications*; Wiley Interscience: New York, 1980.

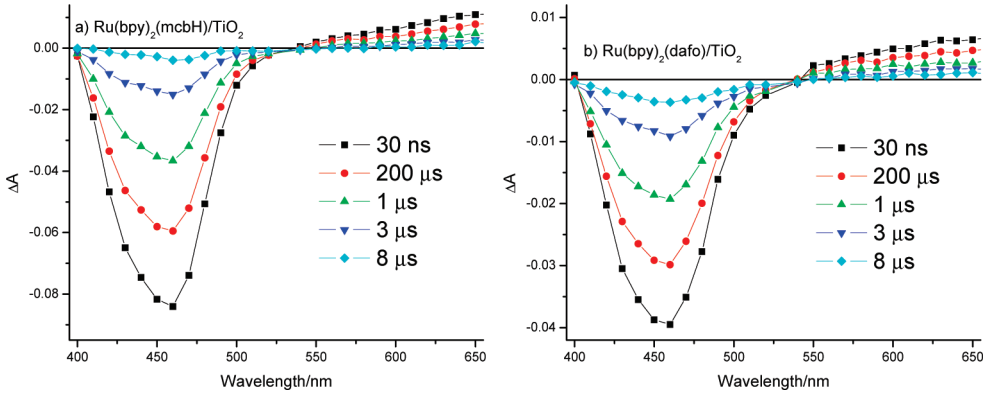

Figure 5. (a) Absorption difference spectra measured at the indicated delay times after pulsed 532 nm light excitation of (a) $Ru(bpy)_2(mcbH)/TiO_2$ and (b) $Ru(bpy)_2(dafo)/TiO_2$ thin films immersed in 0.1 M $LiClO_4$ acetonitrile at room temperature.

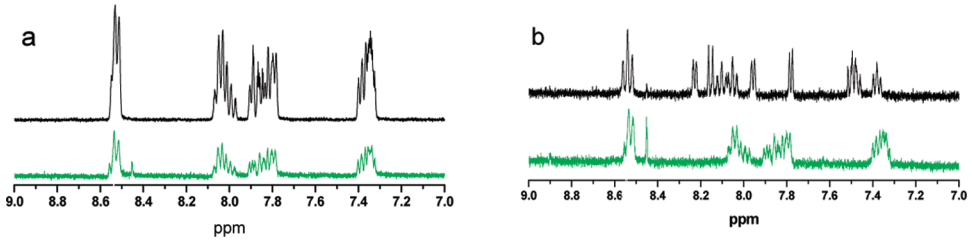

Figure 6. ^1H NMR in pD = 10 NaOD solution in deuterium oxide for (a) $[Ru(bpy)_2(mcbH)](PF_6)_2$, and (b) $[Ru(bpy)_2(dafo)](PF_6)_2$ for authentic samples (top), and that desorbed from TiO_2 (bottom).

The sensitizers were removed from the TiO_2 surface by reacting the sensitized thin films with a basic aqueous solution (pH = 10 NaOH) for 2−3 h. The visible absorption spectrum of the aqueous solution that had been exposed to $Ru(bpy)_2(mcbH)/TiO_2$ was identical to authentic samples of the compound in pH 10 water and were consistent with previous literature reports of the deprotonated carboxylate compound.[17] The absorption spectrum of the aqueous solution exposed to $Ru(bpy)_2(dafo)/TiO_2$ was within experimental error the same as that desorbed from $Ru(bpy)_2(mcbH)/TiO_2$, and the MLCT absorption band was significantly red-shifted from that of $[Ru(bpy)_2(dafo)]^{2+}$ dissolved in a pH = 10 aqueous solution.

Deuterium oxide at pD = 10 was used to desorb the compounds from TiO_2 for subsequent ^1H NMR characterization. The ^1H NMR spectra obtained from the TiO_2 desorbed samples were within experimental error the same for $Ru(bpy)_2(mcbH)/TiO_2$ and $Ru(bpy)_2(dafo)/TiO_2$ and displayed four peak groupings centered at 8.53, 8.04, 7.85, and 7.36 ppm in a 5:5:7:6 integration ratio. An important resonance for the surface chemistry proposed below, was the 3′-H on the reacted dafo ligand that was observed at 8.5 ppm. The ^1H NMR results obtained with an authentic sample of $[Ru(bpy)_2(mcbH)]^{2+}$ were in good agreement with those samples desorbed from TiO_2. There was, however, a significant difference in the spectrum of compounds desorbed from $Ru(bpy)_2(dafo)/TiO_2$ compared with that of a freshly prepared sample of $[Ru(bpy)_2(dafo)]^{2+}$ dissolved in pD = 10 $NaOD/D_2O$ solution, Figure 6b. Furthermore, upon prolonged standing (hours) the NMR spectrum of the latter sample slowly evolved until it was similar to the spectrum of authentic $[Ru(bpy)_2(mcbH)]^{2+}$ recorded in the same solvent mixture. Significant differences noted were a change in the relative integration of the multiplet at 8.5 ppm (assigned to the bpy-3,3′-H and mcbH-3′-H, vide infra) from 5 to 4, and an increase in the splitting of the doublet at 7.96 ppm (assigned to the mcbH-4′-H). These changes are consistent with occurrence of a slow ring-opening reaction of $[Ru(bpy)_2(dafo)]^{2+}$ in pD = 10 D_2O solution, but with incorporation of deuterium into the 3′-position on the mcbH ligand in this case. It is important to note that the observation of the 5:5:7:6 integration ratio for the product desorbed from $Ru(bpy)_2(dafo)/TiO_2$ clearly indicates that the ring-opening reaction in that case occurs on the TiO_2 surface, *prior* to desorption of the sample into the $NaOD/D_2O$ solution.

Authentic samples of $[Ru(bpy)_2(mcbH)]^{2+}$ displayed ^1H NMR spectra that consisted of four multiplets centered around 8.49, 7.99, 7.80, and 7.32 ppm, with relative integrations of 5, 5, 7, and 6 H's, respectively. Owing to the complexity of the peak splitting and overlapping of peaks within each multiplet, the identity of the protons contributing to each multiplet were successfully assigned based upon combined results of 2-D ($^1H-^1H$ COSY and $^1H-^{13}C$ HMQC and HMBC) experiments, see Supporting Information for additional details. In the following assignments, protons on the unsubstituted pyridine ring of the mcb ligand are primed: 8.49 (m, 5 H, bpy 3,3′-H and mcb 3′-H); 7.99 (m, 5 H, bpy 4,4′-H, and mcb 4′-H); 7.80 (m, 7 H, bpy 6,6′-H, mcb 6,6′-H, and mcb 4-H); and 7.32 (m, 6 H, bpy 5,5′-H, mcb 5,5′-H). The ^{13}C spectrum of $[Ru(bpy)_2(mcbH)]^+$ in basic D_2O solution shows the highest-field peak at 174.3 ppm which is assigned to the carboxylate carbon. Key to the above proton assignments was the unambiguous identification of the peak corresponding to the mcb 4-H (the proton on the carbon adjacent to the carbon bearing the carboxylate group) via the $^1H-^{13}C$ HMBC spectrum.

The photocurrent action spectra of the sensitized TiO_2 thin films measured in a sandwich cell arrangement with a Pt

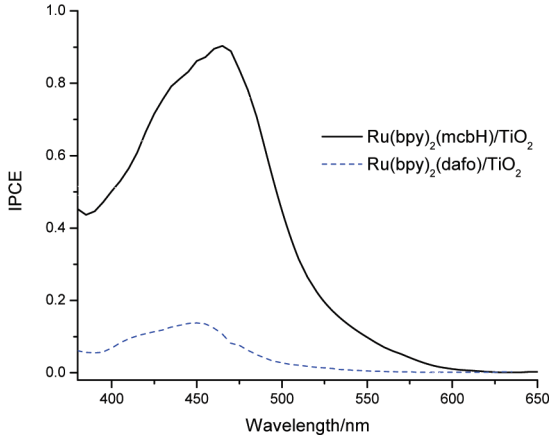

Figure 7. Incident photon-to-current efficiency (IPCE) versus wavelength for $Ru(bpy)_2(mcbH)/TiO_2$ (solid line) and $Ru(bpy)_2(dafo)/TiO_2$ (dashed line) in 0.5 M LiI/0.05 M I_2 acetonitrile solution.

counter electrode and a 0.5 M LiI/0.05 M I_2 CH_3CN electrolyte are shown in Figure 7. The incident-photon-to-current efficiency (IPCE) was significantly lower for $Ru(bpy)_2(dafo)/TiO_2$ than for $Ru(bpy)_2(mcbH)/TiO_2$ at all wavelengths where a significant photocurrent was measured even though the fraction of light absorbed was approximately the same for the two sensitized materials. For $Ru(bpy)_2(dafo)/TiO_2$ thin films that had been pretreated with aqueous acidic solutions, the fraction of light absorbed at the MLCT maximum was about 0.5 but the IPCE was only 0.06. When corrections were made for transmitted light, the absorbed photon-to-current efficiency was 0.13.

Discussion

The reaction of $[Ru(bpy)_2(dafo)]^{2+}$ with TiO_2 resulted in spectroscopic changes consistent with oxidation of the ketone group. The corresponding reaction of $[Ru(bpy)_2(mcbH)]^{2+}$ yielded the expected deprotonation of the carboxylic acid group. The spectroscopic properties of the two sensitized films were remarkably similar and consistent with carboxylate binding to TiO_2. However, the photocurrent measured in regenerative solar cells was significantly larger for films sensitized with $[Ru(bpy)_2(mcbH)]^{2+}$. Below we discuss this reaction chemistry and the implications for solar energy conversion in dye-sensitized solar cells. Note that throughout the text the sensitized films are abbreviated as $Ru(bpy)_2(dafo)/TiO_2$ and $Ru(bpy)_2(mcbH)/TiO_2$ to designate the Ru(II) compound that was reacted with the surface. This should not be confused with the compound actually present on the surface, which is shown to be different.

Chemistry at metal oxide interfaces has often been rationalized by the presence of surface OH groups, Scheme 2.[20] A covalent bond between the oxygen atom and a surface atom is tacitly assumed although an aqueous "gel" layer on the semiconductor surface is also sometimes invoked.[20] In the case of TiO_2, "titanol" groups are often postulated and

Scheme 2

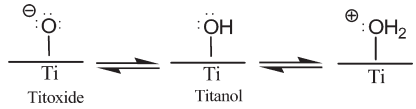

experimental evidence for their existence is compelling.[21−23] The titanol groups undergo acid−base equilibria, and the deprotonated form, by analogy to alcohols, is termed titoxide. McQuillan and co-workers reported infrared studies of nanocrystalline anatase TiO_2 thin films very similar to those utilized for this study.[23] Spectroscopic evidence for the three surface species shown in Scheme 2 were reported as well as a fourth species observed at low pH that was tentatively assigned to protonation of a bridging μ-oxo group. The point of zero charge was determined to occur at a pH of 5.[23] Traditional acid−base titrations of P-25 TiO_2 suspensions allowed determination of the pK_a's for the two equilibria depicted in Scheme 2.[24,25] A complication with this titration data was that the equilibrium constants were sensitive to the concentration of ionizable surface groups present, behavior attributed to electrostatic interaction of charged groups with the leaving protons.[25] Nevertheless, analytical equations were fit to the titration data that allowed the fraction of surface species present an any given pH to be calculated. The surface functionalization chemistry reported here was performed in acetonitrile solutions with TiO_2 thin films that were pretreated with aqueous solutions of pH 12 or 1. On the basis of the previous titration data, at these pH extremes it is expected that there exist negligibly small concentrations of the titoxide (pH 1) or protonated titanol (pH 12), yet with a significant concentration of titanol groups.

Shown in Scheme 3 is a proposed mechanism for the conversion of the ketone group of the coordinated dafo ligand to a carboxylate group observed on base-pretreated TiO_2. The ^1H NMR, UV−visible, ATR-FTIR, and luminescent properties were all consistent with quantitative surface chemistry shown in Scheme 3. The mechanism involves four key steps: (1) coordination of the ketone oxygen to a surface site; (2) nucleophilic attack on the activated C atom of the carbonyl group; (3) ring-opening to yield a carboxylate and a carbanion; and (4) proton transfer to the carbanion to form the observed product. While the molecular-level mechanism(s) remain speculative, the possible surface sites involved in this interfacial reactivity are briefly discussed.

The $[Ru(bpy)_2(dafo)]^{2+}$ reaction with acid-pretreated TiO_2 resulted in coloration of the film but with spectroscopic properties that were within experimental error the same as that for the unreacted compound. This physisorption may involve hydrogen bonding of the carbonyl oxygen to surface titanol groups or weak binding of dafo to unsaturated surface Ti(IV) sites. A weak Ti−O bond is reasonable based on hard−soft acid−base considerations. We note also that $TiCl_4$ has previously been employed as a Lewis acid catalyst to activate the ketone group in Knoevenagel condensation reactions of dafo.[26] The ring-opening chemistry was only observed on base-pretreated TiO_2 which suggests nucleophilic attack at the carbonyl carbon of the coordinated dafo ligand was by a basic titoxide site. Indeed base-catalyzed

(20) Adamson, A. W. *Physical Chemistry of Surfaces*; Wiley Interscience: New York, 1990.
(21) Livage, J.; Henry, M.; Sanchez, C. *Prog. Solid State Chem.* **1988**, *18*, 259.
(22) Gianotti, E.; Dellarocca, V.; Pena, M. L.; Rey, F.; Corma, A.; Coluccia, S.; Marchese, L. *Res. Chem. Intermed.* **2004**, *30*, 871.
(23) Connor, P. A.; Dobson, K. D.; McQuillan, A. J. *Langmuir* **1999**, *15*, 2402.
(24) Boehm, H. P. *Disc. Faraday Soc.* **1971**, *52*, 264.
(25) Schindler, P. W.; Gamsjager, H. *Disc. Faraday Soc.* **1971**, *52*, 286.
(26) Utley, J. H. P.; Ling-Chung, S.-K. *Electrochim. Acta* **1997**, *42*, 2109–2115.

Scheme 3

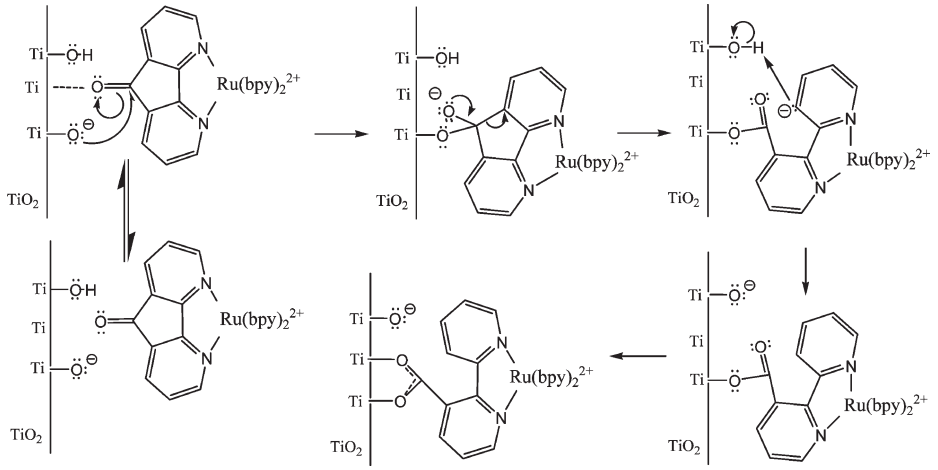

reactions of coordinated dafo ligands in homogeneous fluid solution have previously been documented by Wang and Rillema.[27,28]

Ring-opening forms a surface-bound carboxylate group with a pyridyl anion on the 3′-position of the other pyridine ring. Included in the driving force for this reaction is the strain energy released during rupture of the strained 5-membered ring of the dafo ligand. One measure of this strain energy is the unusually high frequency 1720 cm^{-1} CO stretch observed for the free ligand and 1740 cm^{-1} when coordinated to $Ru(bpy)_2$. In addition, the N−Ru−N bite angle of 81.9° of the dafo ligand[29] relaxes to a more favorable 77° in the coordinated mcbH. The crystallographic data indicate the Ru−N bond to the pyridine ring of the mcbH ligand that is substituted with the carboxylic acid group is also significantly shorter and hence stronger than the other Ru−N bonds. Previous molecular mechanics calculations indicated a 15 kcal/mol decrease in energy when the bite angle about Ru(II) was decreased by this magnitude.[27] The unfavorable bite angle of the dafo ligand is known to stabilize ligand-field excited states that effectively quench the MLCT excited state.[17,30,31] The weak steady-state photoluminescence observed after $[Ru(bpy)_2(dafo)]^{2+}$ reacted with TiO_2 therefore provides indirect evidence for the proposed ring-opening reaction. The putative carbanion was not directly observed, and rapid proton transfer from a titanol group was expected to yield the observed product.

Desorption of the sensitizers from multiple $Ru(bpy)_2(dafo)/TiO_2$ thin films and subsequent ^1H NMR analysis revealed that the expected carboxylate product was indeed formed. Deuterium isotope studies demonstrated that the carboxylate product was not a byproduct of the sensitizer desorption process. Base-catalyzed hydrolysis of $[Ru(bpy)_2(dafo)]^{2+}$ in $NaOD/D_2O$ solution resulted in the selective incorporation of a deuterium atom in the 3′-position of the reacting ligand, whereas for the NaOD desorption studies with TiO_2 a 3′ hydrogen atom was found.

The carboxylate reaction product binds to the surface in concentrations equal to that observed after the reaction of $[Ru(bpy)_2(mcbH)]^{2+}$ with TiO_2. Infrared analysis of the surface-bound sensitizers were very similar; however, the peaks were significantly broader for $Ru(bpy)_2(dafo)/TiO_2$, behavior that may reflect a less uniform distribution of sensitizer environments. The COO asymmetric stretch at 1600 cm^{-1} was the most intense absorption band with a full width at half-maximum (fwhm) of 100 cm^{-1} for $Ru(bpy)_2(dafo)/TiO_2$ compared to 50 cm^{-1} for $Ru(bpy)_2(mcbH)/TiO_2$. The uncertainty in the fwhm for the less intense absorption features was significant, making comparisons more difficult. Nevertheless, all the IR absorptions appeared to be broader for $Ru(bpy)_2(dafo)/TiO_2$ suggesting that the distribution of environments that presumably results from surface heterogeneity was experienced by the entire compound and not restricted to the binding group.

Deacon and Philips have examined the Raman and infrared spectroscopy of X-ray crystallographically characterized metal-carboxylate compounds and found that a correlation exists between the nature of the carboxylate−metal coordination mode and the energy separation between the asymmetric and symmetric COO stretches, $\Delta = \nu_{assym}(CO_2^-) - \nu_{sym}(CO_2^-)$.[18] This same Δ parameter has been previously used as an indirect measure of the surface linkage that results from the reaction of carboxylic acid containing compounds with heterogeneous metal oxide surfaces.[12,31−33] In this study, IR data for both sensitized materials yielded a Δ = 235 cm^{-1}, even though one oxygen atom was derived from the TiO_2 interface in the $[Ru(bpy)_2(dafo)]^{2+}$ reaction. This value is larger than that measured for the carboxylate form of $[Ru(bpy)_2(mcbH)]^{2+}$ and is most consistent with a bridging surface linkage where each carboxylate oxygen is linked to a single surface site, presumably Ti(IV).[18] We note that the nature of the surface binding site remains speculative in this, and previous studies even though titanium−carboxylate compounds are well-known and have recently been characterized by X-ray crystallography.[34,35]

(27) Wang, Y.; Rillema, D. P. *Tetrahedron Lett*. **1997**, *38*, 6627.
(28) Wang, Y.; Rillema, D. P. *Inorg. Chem. Commun*. **1998**, *1*, 27.
(29) Wang, Y.; Jackman, D. C.; Woods, C.; Rillema, D. P. *J. Chem. Crystallogr*. **1995**, *25*, 549.
(30) Henderson, L. J., Jr.; Fronczek, F. R.; Cherry, W. R. *J. Am. Chem. Soc*. **1984**, *106*, 5876.
(31) Wacholtz, W. M.; Auerbach, R. A.; Schmehl, R. H.; Ollino, M.; Cherry, W. R. *Inorg. Chem*. **1985**, *24*, 1758.
(32) Meyer, T. J.; Meyer, G. J.; Pfennig, B. W.; Schoonover, J. R.; Timpson, C. J.; Wall, J. F.; Kobusch, C.; Chen, X.; Peek, B. M.; Wall, C. G.; Ou, W.; Erickson, B. W.; Bignozzi, C. A. *Inorg. Chem*. **1994**, *33*, 3952.
(33) Kilsa, K.; Mayo, E. I.; Brunschwig, B. S.; Gray, H. B.; Lewis, N. S.; Winkler, J. R. *J. Phys. Chem. B* **2004**, *108*, 15640.
(34) Doeuff, S.; Dromzee, Y.; Taulelle, F.; Sanchez, C. *Inorg. Chem*. **1989**, *28*, 4439.

Scheme 4

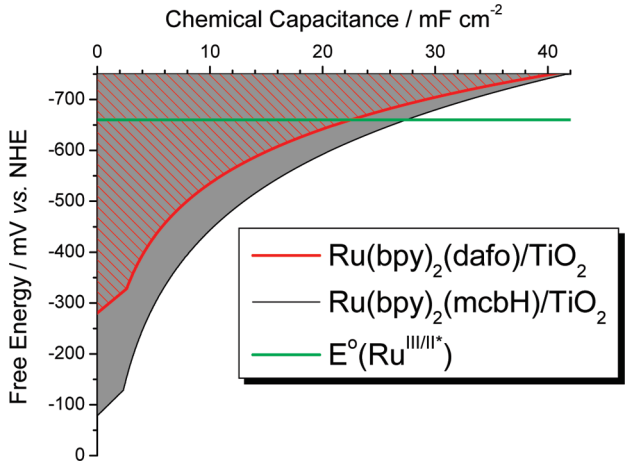

Interestingly, when $Ru(bpy)_2(dafo)/TiO_2$ thin films were utilized in regenerative solar cells, the photocurrent efficiency was about a factor of 4 smaller than that observed for cells prepared with $Ru(bpy)_2(mcbH)/TiO_2$. Likewise, the excited state injection yields measured spectroscopically were consistently 2−3 times lower for $Ru(bpy)_2(dafo)/TiO_2$. These observations were surprising as the spectroscopic properties of the two surface-anchored sensitizers were very similar, and their excited-state reduction potentials were essentially the same, $E_{1/2}(Ru^{III/II*}) = -1.2$ V versus $Ag/AgNO_3$. A possible explanation for the disparate interfacial charge-transfer behavior lies in the TiO_2 functionalization chemistry. The reaction with $[Ru(bpy)_2(mcbH)]^{2+}$ results in proton transfer *to* TiO_2, where the corresponding reaction of $[Ru(bpy)_2(dafo)]^{2+}$ involves OH transfer *from* TiO_2 to the sensitizer. The transfer of protons to TiO_2 is known to stabilize the conduction-band states and favor excited-state injection, behavior consistent with the higher excited-state injection yield and photocurrent of $Ru(bpy)_2(mcbH)/TiO_2$.[35,36]

To test this hypothesis, the sensitized TiO_2 thin films were characterized by spectroelectrochemistry as has been previously described.[37,38] Reduction of the sensitized thin films resulted in the characteristic absorption of electrons trapped in TiO_2. The absorption reported directly on the concentration of trap states that was expressed as a chemical capacitance as a function of free energy. The data was converted to the normal hydrogen electrode (NHE) scale so that it could be compared with the sensitizer excited-state reduction potential, $E_{1/2}(Ru^{III/II*})$, that was found to be within experimental error the same for the two sensitizers, Scheme 4. This data does indeed show that the onset of the redox active TiO_2 states was significantly more positive for $Ru(bpy)_2(mcbH)/TiO_2$ *and* that a larger density of states exists at $E_{1/2}(Ru^{III/II})$. Gerischer theory indicates that the injection rate constant is proportional to the overlap of the excited-state sensitizer donor levels with the unfilled states of TiO_2.[39−41]

It is difficult to conclude whether the trap state distribution for the two sensitized materials is in itself sufficient to explain the factor of 2−3 change in injection yields measured spectroscopically. To our knowledge, analysis of this type to quantify injection yields has not been previously reported and was restricted to the influence adsorbates had on the open circuit photovoltage.[42] Nevertheless, the data in Scheme 4 do help rationalize the transient absorption and photoelectrochemical behaviors. The previously mentioned perylene anhydride compound presumably undergoes surface chemistry similar to that proposed for $[Ru(bpy)_2(dafo)]^{2+}$, but the singlet excited state of peryelene is a potent photoreductant expected to have a stronger overlap with TiO_2 consistent with the high photocurrents reported.[13,14] The injection yield and photocurrent efficiency observed for $Ru(bpy)_2(mcbH)/TiO_2$ in the blue absorption region are in fact notably high, particularly for a compound with a single carboxylic acid group.[33] It will be of interest to examine whether Ru(II) isothiocyante compounds based on terpyridyl or bipyridyl with a single carboxylic acid group in the 3 position would also sensitize TiO_2 efficiently but across a larger portion of the visible region.[8,9]

Conclusions

The reaction of $[Ru(bpy)_2(dafo)]^{2+}$ with a nanocrystalline mesoporous TiO_2 thin film in acetonitrile resulted in interfacial chemistry. Comparative studies with $[Ru(bpy)_2(mcbH)]^{2+}$ support a proposed ring-opening reaction of the Ru^{II}-coordinated dafo ligand that ultimately yields a 3-carboxylate-2,2′-bipyridine ligand bound to the TiO_2 surface. The spectroscopic properties of $Ru(bpy)_2(dafo)/TiO_2$ and $Ru(bpy)_2(mcbH)/TiO_2$ were very similar, although the excited-state injection yield measured on a nanosecond time scale was consistently lower for the former. In regenerative photoelectrochemical solar cells, the incident photon-to-current efficiency (IPCE) was significantly lower for $Ru(bpy)_2(dafo)/TiO_2$, behavior that presumably reflects the same lower excited-state injection yield measured spectroscopically.

Acknowledgment. The National Science Foundation is gratefully acknowledged for research support. M.A. thanks the Swedish Research Council for a personal postdoctoral research Grant 623-2007-1038. W.B.H. acknowledges support from the Naval Academy Research Council.

Supporting Information Available: Further details are given on the 2-D NMR spectra used to assign ^1H NMR resonances. This material is available free of charge via the Internet at http://pubs.acs.org.

(35) Uppal, R.; Incarvito, C. D.; Lakshmi, K. V.; Valentine, A. M. *Inorg. Chem.* **2006**, *45*, 1795.
(36) Liu, F.; Meyer, G. J. *Inorg. Chem.* **2003**, *42*, 7351.
(37) Morris, A. J.; Meyer, G. J. *J. Phys. Chem. C* **2008**, *112*, 18224.
(38) Fabregat-Santiago, F.; Mora-Sero, I.; Garcia-Belmonte, G.; Bisquert, J. *J. Phys. Chem. B* **2003**, *107*, 758.
(39) Gerischer, H. *Surf. Sci.* **1969**, *18*, 97.
(40) Gerischer, H. *Photochem. Photobiol.* **1972**, *16*, 243.
(41) Gerischer, H.; Willig, F. *Top. Curr. Chem.* **1976**, *61*, 31.
(42) Zhang, Z.; Zakeeruddin, S. M.; O'Regan, B. C.; Humphry-Baker, R.; Grätzel, M. *J. Phys. Chem. B* **2005**, *109*, 21818.